A Highly Fluorescent σ - Bonded Platinum(II) Diketopyrrolopyrrole Complex

Kamioka, Misaki
Department of Chemistry and Biochemistry, Graduate School of Engineering, Kyushu University

Wang, Yitong
Department of Chemistry and Biochemistry, Graduate School of Engineering, Kyushu University

Mori, Shigeki
Advanced Research Support Center (ADRES) Ehime University

Furuta, Hiroyuki
Department of Chemistry and Biochemistry, Graduate School of Engineering, Kyushu University

他

https://hdl.handle.net/2324/7181922

出版情報：European Journal of Inorganic Chemistry. 2022 (14), pp.e202200081-, 2022-05-02. Wiley
バージョン：

Highly Fluorescent σ-Bonded Platinum(II) Diketopyrrolopyrrole Complex

Misaki Kamioka,[a] Yitong Wang,[a] Shigeki Mori,[b] Hiroyuki Furuta*[a] and Soji Shimizu*[a]

[a] M. Kamioka, Y. Wang, Prof. Dr. H. Furuta, Prof. Dr. S. Shimizu
Department of Chemistry and Biochemistry, Graduate School of Engineering and Center for Molecular Systems (CMS)
Kyushu University
Fukuoka 819-0395 (Japan)
E-mail: hfuruta@cstf.kyushu-u.ac.jp, ssoji@cstf.kyushu-u.ac.jp
[b] Dr. S. Mori
Advanced Research Support Center (ADRES)
Ehime University
Matsuyama 790-8577 (Japan)

Supporting information for this article is given via a link at the end of the document.

Abstract: A σ-bonded platinum(II) diketopyrrolopyrrole (Pt-DPP) complex was synthesized from a reaction of *p*-pinacolatoborylphenyl-substituted DPP with dichloro(1,5-cyclooctadiene)platinum(II), followed by a ligand exchange reaction with triphenylphosphine. The Pt-DPP complex is highly fluorescent not only in solution but also in the solid state. From the comparison of the emission properties with those of *N*-benzyl-DPPs bearing phenyl and *p*-bromophenyl substituents, the intense emission of the Pt-DPP complex is ascribed to the DPP-centered fluorescence. In the solid state, aggregation-caused quenching is mitigated by the well-segregated molecular packing due to the bulky triphenylphosphine ligands. The facile synthesis and unique fluorescence properties of the Pt-DPP complex are beneficial for creating DPP-based functional chromophores.

Introduction

Diketopyrrolopyrrole (DPP),[1,2] a conventional red pigment, has widely been used as a functional chromophore in various research fields, such as bioimaging and light-mediated therapy,[3] owing to its intense absorption and fluorescence in the visible region. The electron-accepting nature inherent to the lactam moieties of DPP has also enabled its use as an acceptor unit[4] in creating donor-acceptor small molecules and polymers for organic transistors and photovoltaics.[5–8] Extension of the π-conjugated system of DPP has also been intensively investigated to control the optical properties in the far-red and near-infrared regions.[9–11] To prevent aggregation caused by intermolecular hydrogen-bonding interactions and π-π stacking, *N*-alkylation of DPPs has frequently been conducted in the application studies mentioned above (Figure 1). Although prominent optical properties in solution can be attained by *N*-alkylation, it is not the case with those in the solid state. Kanbara *et al*. reported the optical properties of *N*-benzyl-substituted DPPs with four different kinds of *para*-substituted aryl groups.[12] All the compounds exhibited fluorescence with high fluorescence quantum yields (0.86–0.91) in solution. In contrast, the fluorescence emission in the solid state was virtually quenched, except for DPP with 4-butoxyphenyl substituents, which exhibited moderately intense fluorescence in the solid state with a quantum yield of 0.45. They explained that the larger Stokes shift than those of the other DPPs could prevent fluorescence quenching caused by the self-absorption in the solid state. The solid-state emission of DPP can also be achieved by *N*-metalation with transition metal ions bearing bulky triphenylphosphine ligands (**DPP-M-1**, Figure 1).[13] Despite the presence of heavy atoms, these *N*-metalated DPP complexes exhibit rather intense fluorescence both in solution and solid states. In contrast, fluorescence quenching due to the heavy atom effect is significant for **DPP-M-2**, in which a platinum ion is coordinated by an *o*-pyridyl group in addition to the lactam nitrogen atom.[14] Here, we report the synthesis and solid-state emission behavior of another type of σ-bonded platinum(II)-DPP (Pt-DPP) complex, which possesses bis(triphenylphosphine)platinum(II) chloride at the *para*-position of the phenyl groups. To reveal the origin of its intense solid-state emission, the fluorescence properties in solution and the solid state were compared with those of non-metalated *N*-benzyl-DPP bearing phenyl (**1**, Figure 1) and *p*-bromophenyl groups.

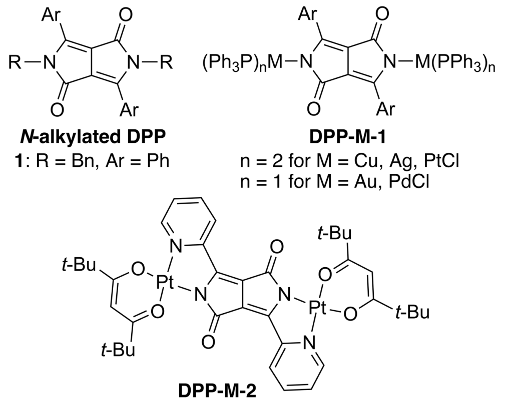

Figure 1. Structures of *N*-alkylated and *N*-metalated DPPs in the literature.

Results and Discussion

The Pt-DPP complex was synthesized as shown in Scheme 1. *p*-Bromophenyl-substituted *N*-benzyl DPP (**2**) reacted with bis(pinacolate)diborane in the presence of bis(triphenylphosphine)palladium(II) dichloride and potassium acetate in 1,4-dioxane at 90 ºC to afford *p*-borylated DPP (**3**) in

75% yield. **3** was converted into the Pt-DPP complex (**4**) in 55% yield by a reaction with two mole equivalents of dichloro(1,5-cyclooctadiene)platinum(II) (Pt(cod)Cl$_2$), followed by a ligand exchange reaction with triphenylphosphine.

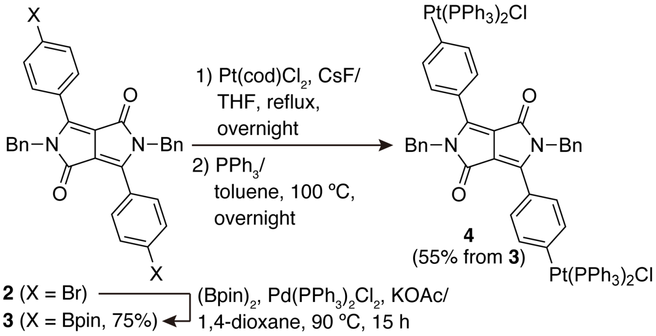

Scheme 1. Synthesis of the σ-bonded Pt-DPP complex (**4**).

The ^{1}H NMR spectrum of **4** in CD$_2$Cl$_2$ exhibits a simple signal pattern owing to the twofold molecular symmetry of **4** (Figure S8). Two signals at 6.82 and 6.50 ppm, which are assigned to the platinum-coordinated phenyl protons, are upfield shifted due to the diatropic ring current effect of the benzene rings of the triphenylphosphine ligands. The structure of **4** was unambiguously elucidated by single crystal X-ray diffraction analysis (Figure 2).[15] Each platinum(II) ion is coordinated by one chloride, one phenyl group of DPP, and two triphenylphosphine ligands. The phenyl groups of DPP are sandwiched by the triphenylphosphine ligands, consistent with the upfield shifts of these proton signals in the ^{1}H NMR spectrum of **4**. In the molecular packing, each molecule is loosely slip-stacked in a parallel manner with a center-to-center distance of 11.1 Å due to the steric hindrance of the bulky triphenylphosphine ligands and *N*-benzyl groups (a center denotes centroid of the fused five-membered rings of the DPP core as shown in Figure 2b).

In the UV/vis absorption spectrum of **4** in chloroform, two bands are observed at 503 and 350 nm (Figure 3 and Table 1). The spectral profile is broadly similar to those of **1** and **2**, and the main band at 503 nm is slightly red-shifted. To give a detailed insight into the absorption spectra, the time-dependent (TD) DFT calculations were performed on model structures (**1M**, **2M**, and **4M**), in which *N*-benzyl groups were replaced with *N*-methyl groups for simplicity, at the M06/SDD level (Tables S1–S3). The lowest-energy band comprises the HOMO-to-LUMO transition (**1M**: 464 nm (oscillator strength (*f*) = 0.43), **2M**: 478 nm (*f* = 0.56), and **4M**: 480 nm (*f* = 0.78)). Because both the HOMO and LUMO of **4M** are localized on the DPP moiety (Figure 4), the observed absorption band at 503 nm can be ascribed to a DPP-centered π-π* transition. The TDDFT calculation also reveals the less intense band of **4M** at 360 nm with *f* = 0.10, mainly comprising the transition from the HOMO–2 to the LUMO. This theoretical band can be assigned to the absorption band at 350 nm. Considering that the HOMO–2 is localized on the platinum centers, and **1** and **2** do not exhibit absorption in this region, this band can be ascribed to a metal-to-ligand charge transfer band.

In chloroform, **4** exhibits intense emission at 553 nm with a vibronic shoulder (Figure 3 and Table 1). The lifetime of this photoluminescence is 3.9 ns, indicative of its origin as not phosphorescence but fluorescence. The fluorescence quantum yield of **4** (0.86) is similar to **1** (0.91) and **2** (0.87). The negligible difference in the fluorescence quantum yields indicates the minor heavy atom effects of the bromine and platinum atoms at the *para*-position of the phenyl substituents. This can be explained in terms of the small mixing of the platinum-based d_{xy} orbital with the DPP-based molecular orbitals (MOs) in both the HOMO and LUMO, which can deteriorate the intersystem crossing to the triplet states (Figure 4).

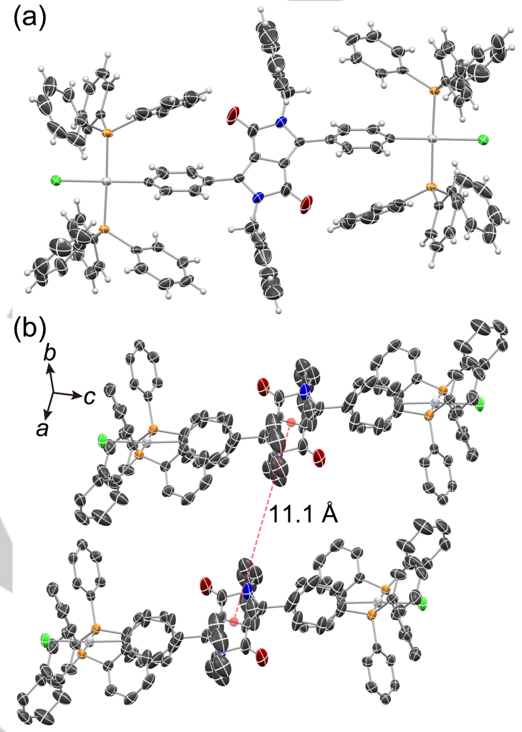

Figure 2. X-ray single crystal structure of **4**. Each of the *N*-benzyl groups is disordered in two positions. One with a larger occupancy is shown. The thermal ellipsoids are scaled to the 50% probability level. (a) Top view and (b) a packing structure, in which the centers are shown by the red dots and connected with a red dashed line. Hydrogen atoms are omitted for clarity in Figure 2b.

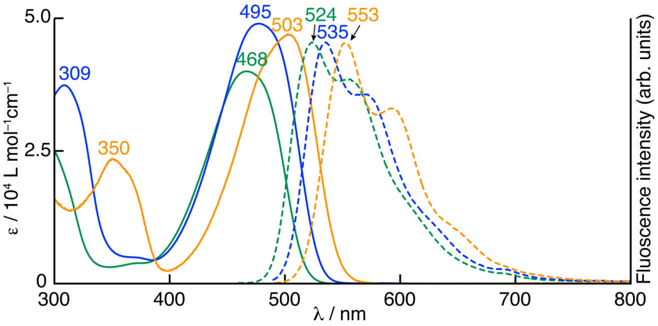

Figure 3. UV/vis absorption (solid lines) and fluorescence (dotted lines) spectra of **1** (green line), **2** (blue line), and **4** (orange line) in CHCl$_3$.

In the solid state, intense emission was observed for **1** and **4**, whereas the emission of **2** was virtually quenched (Figure 5). The fluorescence quantum yields in powder are moderately high, 0.20 for **1** and 0.45 for **4**. The observed difference in the solid-state emission between **1** and **2** can be rationalized by the larger

Stokes shift of **1** (2280 cm^{-1}) than that of **2** (1510 cm^{-1}), which can alleviate self-absorption quenching. Despite the moderate Stokes shift of **4** (1780 cm^{-1}), the fluorescence quantum yield is even higher than **1**. This is not only due to the small overlap between the absorption and fluorescence spectra but also due to the well-segregated molecular packing of **4** as observed in the crystal structure, which can prevent self-absorption quenching.

Table 1. Photophysical properties of **1**, **2**, and **4**.

Compound	State	λ_{max}^{Abs} [nm]	λ_{max}^{Fl} [nm]	Stokes shift [cm^{-1}]	Φ	τ [ns]
1	solution[a]	468	524	2280	0.91	3.8
	solid[b]	485	620	4490	0.20	–
2	solution[a]	495	535	1510	0.87	4.2
	solid[b]	501	628	4040	0.05	–
4	solution[a]	503	553	1780	0.86	3.9
	solid[b]	506	606	3260	0.45	–

[a] In $CHCl_3$ solution. [b] UV/vis absorption and fluorescence spectra were measured in a drop-cast film state. Fluorescence quantum yields were measured in a powder. Fluorescence lifetimes in the solid state were not measured.

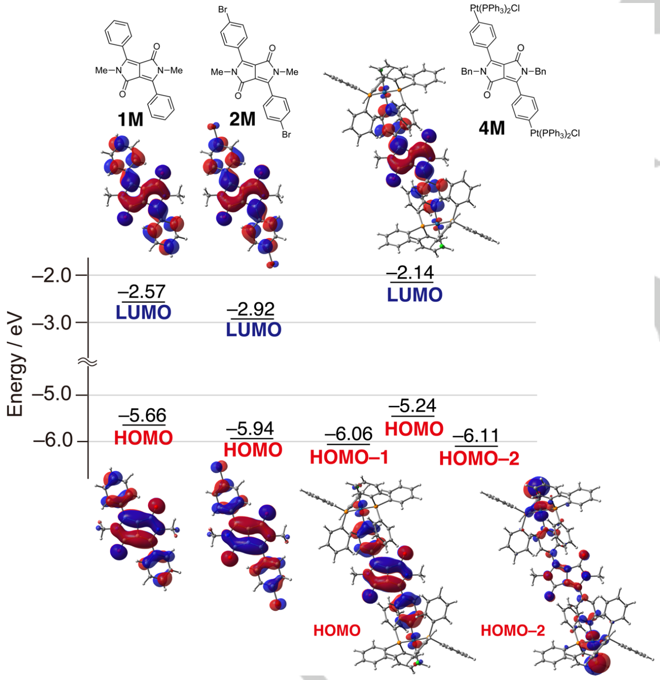

Figure 4. Partial frontier MO diagram of **1M**, **2M**, and **4M** at the M06/SDD level. HOMO–2 of **4M** is also shown. Detailed MO diagrams are shown in Figures S12–14 in the Supporting Information.

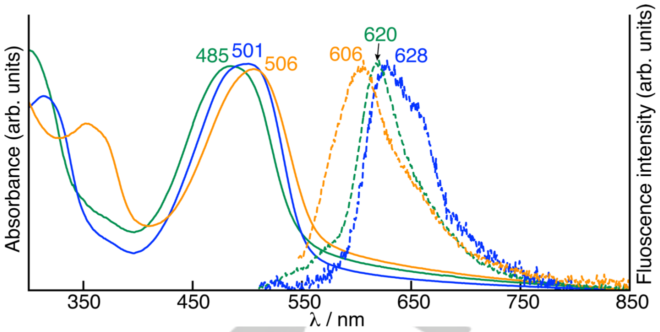

Figure 5. UV/vis absorption (solid lines) and fluorescence (dotted lines) spectra of **1** (green line), **2** (blue line), and **4** (orange line) in drop cast films.

Cyclic voltammograms of **1**, **2**, and **4** were measured in *o*-dichlorobenzene containing tetra-*n*-butylammonium perchlorate (0.1 M) as a supporting electrolyte (Figure 6). All the compounds exhibit irreversible or pseudo-reversible oxidation and reversible reduction waves. A cathodic shift of the oxidation potential is observed for **4** (0.31 V vs. Fc$^+$/Fc) compared with **1** (0.71 V) and **2** (0.77 V), whereas the reduction potentials exhibit anodic shifts on going from **1** (–1.71 V), **2** (–1.56 V), and **4** (–1.43 V). The potential difference value (ΔE) between the oxidation and reduction potentials thus decreases from **1** (2.42 V) and **2** (2.33 V) to **4** (1.74 V), which is in good agreement with the red-shifts of the absorption spectra in this order.

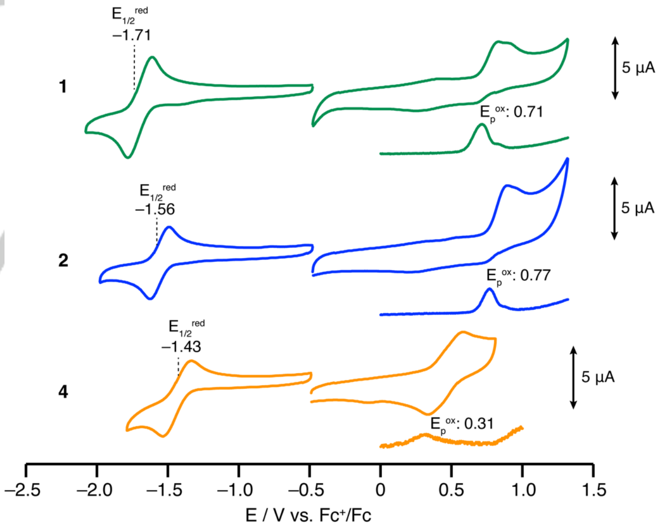

Figure 6. Cyclic voltammograms (CV) and differential pulse voltammograms (DPV) of **1** (green lines), **2** (blue lines), and **4** (orange lines) in *o*-dichlorobenzene containing tetra-*n*-butylammonium perchlorate (0.1 M) at a scan rate of 100 mV s^{-1}.

Conclusion

In summary, the σ-bonded platinum(II) complex of DPP bearing *N*-benzyl groups was synthesized, and its fluorescence properties in solution and solid states were investigated. Despite the presence of the heavy platinum atoms, the Pt-DPP complex exhibits fluorescence owing to the minor mixing of the platinum-based d_{xy} orbital with the DPP-based frontier MOs, which diminishes the intersystem crossing to triplet states. The solid-state emission of the Pt-DPP complex is also noticeable considering the small Stokes shift, which generally causes the self-absorption quenching in the aggregated state. In the current case, the bulky triphenylphosphine ligands on the platinum(II) atoms prevent mutual stacking of the DPP chromophore, alleviating aggregation-caused quenching. The molecular design for solid-state emission in this study can further be applied to create DPP-based functional chromophore systems toward bioimaging and optoelectronic applications. The research along these directions is being intensively investigated in our laboratory.

Experimental Section

σ-Bonded platinum(II)-DPP complex (4): A solution of **3** (20.0 mg, 27.8 μmol), dichloro(1,5-cyclooctadiene)platinum(II) (20.8 mg, 55.5 μmol), and CsF (25.3 mg, 167 μmol) in THF (1.4 mL) was stirred at reflux overnight under nitrogen atmosphere. The reaction mixture was added to water and extracted with dichloromethane. The organic layer was washed with brine, dried over anhydrous Na_2SO_4, and concentrated in vacuo. The residue and an excess amount of triphenylphosphine (72.9 mg, 278 μmol) was dissolved in toluene (1.4 mL), and the mixture was stirred overnight at 100 °C. After cooling to room temperature, the solvent was removed under vacuum. The crude mixture was purified by silica gel column chromatography (CH_2Cl_2/AcOEt = 14:1 (v/v)) to provide **4** (30 mg, 55%). ^1H NMR (495 MHz, CD_2Cl_2, 298 K): $\delta = 7.53$ (dd, $J_1 = 12.4$ Hz, $J_2 = 5.9$ Hz, 24H), 7.33–7.23 (m, 42H), 7.10 (d, $J = 7.6$ Hz, 4H), 6.82 (d, $J = 8.3$ Hz, 4H), 6.50 (d, $J = 8.3$ Hz, 4H), 4.70 ppm (s, 4H); ^{13}C NMR (125 MHz, CD_2Cl_2, 298 K): $\delta = 162.9$, 149.3, 139.1, 137.7, 135.1, 130.6, 130.3, 130.1, 128.9, 128.3, 127.6, 127.3, 126.4, 121.1, 108.1, 45.7 ppm; ^{31}P NMR (200 MHz, CD_2Cl_2, 298 K): $\delta = 24.7$ ppm (s, $J_{PtP} = 3094$ Hz); UV/vis ($CHCl_3$): λ_{max} (ε) = 350 (23000), 503 nm (47000 $M^{-1}cm^{-1}$); HRMS (FAB): m/z calcd. for $C_{104}H_{82}Cl_2N_2O_2P_4Pt_2$ = 1974.4000 $[M]^+$; found 1974.4048.

Acknowledgements

This work was supported by Grants-in-Aids for Challenging Research (Exploratory) (JSPS Grant Number 18K19081) and Scientific Research (B) (JSPS KAKENHI Grant Number JP19H02703).

Keywords: Diketopyrrolopyrrole • Platinum(II) complex • Solid-state emission • Fluorescence • σ-Complex

[1] a) A. Iqbal, M. Jost, R. Kirchmayr, J. Pfenninger, A. Rochat, O. Wallquist, *Bull. Soc. Chim. Belg.* **1988**, *97*, 615–643; b) Z. M. Hao, A. Iqbal, *Chem. Soc. Rev.* **1997**, *26*, 203–213; c) J. S. Zambounis, Z. Hao, A. Iqbal, *Nature* **1997**, *388*, 131–132.

[2] For comprehensive reviews about diketopyrrolopyrrole, see: a) M. Grzybowski, D. T. Gryko, *Adv. Opt. Mater.* **2015**, *3*, 280–320; b) Y. Patil, R. Misra, *Chem. Rec.* **2020**, *6*, 596–603.

[3] M. Kaur, D. H. Choi, *Chem. Soc. Rev.* **2015**, *44*, 58–77.

[4] a) A. Purc, E. M. Espinoza, R. Nazir, J. J. Romero, K. Skonieczny, A. Jeżewski, J. M. Larsen, D. T. Gryko, V. I. Vullev, *J. Am. Chem. Soc.* **2016**, *138*, 12826–12832; b) M. Krzeszewski, E. M. Espinoza, C. Červinka, J. B. Derr, J. A. Clark, D. Borchardt, G. J. O. Beran, D. T. Gryko, V. I. Vullev, *Angew. Chem. Int. Ed.* **2018**, *57*, 12365–12369; *Angew. Chem.* **2018**, *130*, 12545–12549.

[5] W. Li, K. H. Hendriks, M. M. Wienk, R. A. J. Janssen, *Acc. Chem. Res.* **2016**, *49*, 78–85.

[6] C. B. Nielsen, M. Turbiez, I. McCulloch, *Adv. Mater.* **2013**, *25*, 1859–1880.

[7] S. Qu, H. Tian, *Chem. Commun.* **2012**, *48*, 3039–3051.

[8] B. Tieke, A. R. Rabindranath, K. Zhang, Y. Zhu, *Beilstein J. Org. Chem.* **2010**, *6*, 830–845.

[9] a) G. M. Fischer, A. P. Ehlers, A. Zumbusch, E. Daltrozzo, *Angew. Chem. Int. Ed.* **2007**, *46*, 3750–3753; *Angew. Chem.* **2007**, *119*, 3824–3827; b) G. M. Fischer, E. Daltrozzo, A. Zumbusch, *Angew. Chem. Int. Ed.* **2011**, *50*, 1406–1409; *Angew. Chem.* **2011**, *123*, 1442–1445; c) G. M. Fischer, M. Isomäki–Krondahl, I. Göttker–Schnetmann, E. Daltrozzo, A. Zumbusch, *Chem. Eur. J.* **2009**, *15*, 4857–4864; d) M. Y. Berezin, W. J. Akers, K. Guo, G. M. Fischer, E. Daltrozzo, A. Zumbusch, S. Achilefu, *Biophys. J.* **2009**, *97*, L22–L24; e) G. M. Fischer, C. Jüngst, M. Isomäki–Krondahl, D. Gauss, H. M. Möller, E. Daltrozzo, A. Zumbusch, *Chem. Commun.* **2010**, *46*, 5289–5291; f) W. J. Akers, C. Kim, M. Berezin, K. Guo, R. Fuhrhop, G. M. Lanza, G. M. Fischer, E. Daltrozzo, A. Zumbusch, X. Cai, L. V. Wang, S. Achilefu, *ACS nano* **2011**, *5*, 173–182; g) G. M. Fischer, M. K. Klein, E. Daltrozzo, A. Zumbusch, *Eur. J. Org. Chem.* **2011**, *2011*, 3421–3429; h) S. Wiktorowski, G. M. Fischer, M. J. Winterhalder, E. Daltrozzo, A. Zumbusch, *PCCP.* **2012**, *14*, 2921–2928.

[10] a) K. Skonieczny, I. Papadopoulos, D. Thiel, K. Gutkowski, P. Haines, P. M. McCosker, A. D. Laurent, P. A. Keller, T. Clark, D. Jacquemin, D. M. Guldi, D. T. Gryko, *Angew. Chem. Int. Ed.* **2020**, *59*, 16104–16113; *Angew. Chem.* **2020**, *132*, 16238–16247; b) K. Gutkowski, K. Skonieczny, M. Bugaj, D. Jacquemin, D. T. Gryko, *Chem. Asian J.* **2020**, *15*, 1369–1375; c) T. Kim, W. Kim, O. Vakuliuk, D. T. Gryko, D. Kim, *J. Am. Chem. Soc.* **2020**, *142*, 1564–1573; d) M. Grzybowski, V. Hugues, M. Blanchard–Desce, D. T. Gryko, *Chem. Eur. J.* **2014**, *20*, 12493–12501.

[11] a) S. Shimizu, *Chem. Commun.* **2019**, *55*, 8722–8743; b) S. Shimizu, T. Iino, Y. Araki, N. Kobayashi, *Chem. Commun.* **2013**, *49*, 1621–1623; c) S. Shimizu, T. Iino, A. Saeki, S. Seki, N. Kobayashi, *Chem. Eur. J.* **2015**, *21*, 2893–2904; d) R. Feng, N. Sato, M. Nomura, A. Saeki, H. Nakanotani, C. Adachi, T. Yasuda, H. Furuta, S. Shimizu, *Journal of Materials Chemistry C* **2020**, *8*, 8770–8776; e) R. Feng, N. Sato, T. Yasuda, H. Furuta, S. Shimizu, *Chem. Commun.* **2020**, *56*, 2975–2978; f) R. Ishimatsu, H. Shintaku, Y. Kage, M. Kamioka, S. Shimizu, K. Nakano, H. Furuta, T. Imato, *J. Am. Chem. Soc.* **2019**, *141*, 11791–11795; g) Y. Kage, H. Karasaki, S. Mori, H. Furuta, S. Shimizu, *ChemPlusChem* **2019**, *84*, 1648–1652; h) Y. Kage, S. Mori, M. Ide, A. Saeki, H. Furuta, S. Shimizu, *Mater. Chem. Front.* **2018**, *2*, 112–120.

[12] J. Kuwabara, T. Yamagata, T. Kanbara, *Tetrahedron* **2010**, *66*, 3736–3741.

[13] a) H. Langhals, M. Limmert, I.-P. Lorenz, P. Mayer, H. Piotrowski, K. Polborn, *Eur. J. Inorg. Chem.* **2000**, *2000*, 2345–2349; b) I.–P. Lorenz, M. Limmert, P. Mayer, H. Piotrowski, H. Langhals, M. Poppe, K. Polborn, *Chem. Eur. J.* **2002**, *8*, 4047–4055.

[14] T. Yamagata, J. Kuwabara, T. Kanbara, *Tetrahedron* **2014**, *70*, 1451–1457.

[15] <url href="<url>https://www.ccdc.cam.ac.uk/services/structures?id=doi:10.1002/chem.202######">Deposition Number 2130624 (for **4**) </url> contains the supplementary crystallographic data for this paper. These data are provided free of charge by the joint Cambridge Crystallographic Data Centre and Fachinformationszentrum Karlsruhe Access Structures service <url href="https://www.ccdc.cam.ac.uk/structures/?">www.ccdc.cam.ac.uk/structures</url>.

Entry for the Table of Contents

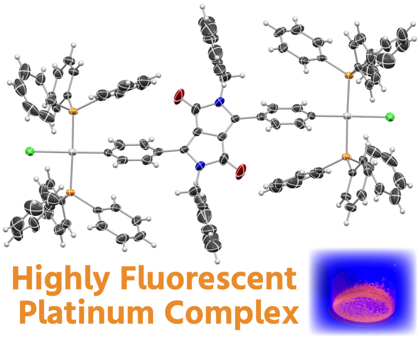

Heavy, but fluorescent: A σ-bonded platinum(II) diketopyrrolopyrrole (Pt-DPP) complex was synthesized. The Pt-DPP complex exhibits intense DPP-centered fluorescence not only in solution but also in the solid state. The solid-state emission is ascribed to the well-segregated molecular packing, mitigating aggregation-caused quenching. The unique fluorescence properties are beneficial for creating DPP-based functional chromophores.